A stochastic B-spline wavelet on the interval finite element method for elastic buckling of columns

***Shashank Vadlamani[1] and †Arun C.O.[1]**

[1]Department of Aerospace Engineering, Indian Institute of Space Science and Technology, Thiruvananthapuram, Kerala-695547, India

*Presenting author: shashankvadlamani@gmail.com
†Corresponding author: shashankvadlamani@gmail.com

Abstract

The current paper presents the solution of elastic buckling of columns using stochastic B-spline wavelet on the interval (BSWI) based wavelet finite element method (WFEM). In this work, the spatial variation of modulus of elasticity is modelled as a homogenous random field. BSWI scaling functions are used for the discretization of the random field. Columns under different boundary conditions are considered as numerical examples. The stochastic Eigen value problem is solved for the response statistics of buckling load with perturbation approach and the results are validated using Monte Carlo simulation (MCS). A parametric study is carried out by considering different coefficient of variation values by varying the standard deviation. A comparative study of computational time needed for the execution of perturbation approach and MCS is also done.

Keywords: B-spline wavelet on the interval; Multiresolution analysis; Random field; Auto-covariance function; Perturbation method; Monte Carlo simulation; Elastic buckling

Introduction

Buckling is one of the predominant modes of failure which is observed when a structure is subjected to an axial compressive type external loading. It is a stability failure wherein, the entire structure collapses suddenly and the critical value of the applied external load causing this failure depends on the geometry of the structure and the stiffness of the material but not its strength [1]. Engineering structures have a high degree of uncertainty associated with its material properties, loads, geometry, operating environments, etc. [2]. The uncertainty in the design parameters will also result in uncertainty in buckling loads and its mode shapes. Therefore, a stochastic modelling approach leads to a robust design by providing additional statistical information on the stability of the structures. At the same time, a stochastic modelling also increases the complexity of the mathematical model and needs a higher computational effort to obtain the system response when compared with a deterministic approach. Nonetheless, widespread research has gone into the development of stochastic based numerical methods over the past few decades due to the availability of powerful computational resources.

Extensive research has gone into the development of stochastic finite element methods (SFEM) [3], wherein a stochastic mesh is generated to discretize the input random field and calculate the response statistics. Vanmarcke and Grigoriu [4] analysed simple beams with random elastic moduli using SFEM. Lin [5] developed a SFEM for the buckling analysis of frames with random initial imperfections, uncertain sectional and material properties. However, due to the high mesh dependency of finite element method (FEM), mapping the random field discretization onto response discretization becomes difficult. Hence, there is a

need for the development of stochastic based numerical methods, which can address the mesh dependency and re-meshing issues of FEM. Meshfree methods have been used in the stochastic analysis [6,7] to alleviate the mesh dependency of FEM. Gupta and Arun [8] proposed a stochastic meshfree method for elastic buckling of columns. In addition to meshfree methods wavelet finite element method (WFEM) is another alternate numerical tool which has shown to reduce the issues related to FEM considerably.

Wavelets are mathematical functions that are used in the approximation of other unknown functions at different levels of resolution. The multiresolution analysis (MRA) and two scale relation properties of wavelets lead to the development of a hierarchy of solutions during the approximation process. Wavelets have a scale varying local basis functions having a compact support that leads to a refinement of solution locally in the regions of high gradient. Therefore, issues related to slow convergence and re-meshing can be addressed using wavelet based numerical methods. B-spline wavelet on the interval (BSWI) has gained widespread popularity from among different wavelets that exist in the literature [9], due to its underlying properties [10,11] and hence, it is selected to be used in the current paper.

One-dimensional (1D) C_0 and C_1 BSWI elements for structural analysis using BSWI WFEM were constructed by Xiang et al. [12]. Deterministic buckling analysis of functionally graded beams and functionally graded plates was done by Zuo et al. in their papers [13] and [14] respectively. Yang et al. [15] carried out a deterministic study of free vibration and buckling analysis of plates.

Besides the discretization of random field, evaluation of response statics also needs to be computationally efficient. Monte Carlo simulation (MCS) has been used for the calculation of response statistics. Elishakoff [16] solved the problem of buckling of finite columns with initial imperfections, resting on a softening nonlinear elastic foundation by Monte Carlo method. But the usage of MCS makes the modelling process computationally expensive with increase in MCS sample size and number of random variables. Hence, a more viable procedure is needed that requires less computational effort. In this regard, perturbation methods have been extensively used for SFEM or stochastic meshless methods.

From the existing literature, it is noticed that a stochastic BSWI WFEM formulation for elastic buckling of columns using the perturbation method for calculating the response statistics, while material properties are modelled as random field does not exist. Hence, in the present study, the solution of elastic buckling of columns using stochastic BSWI WFEM is presented. The spatial variation of modulus of elasticity is modelled as a homogenous random field. BSWI scaling functions are used for the discretization of the random field and response. Columns under different boundary conditions are considered as numerical examples. The stochastic Eigen value problem is solved for the response statistics of buckling load with perturbation approach and the results are validated using MCS. A parametric study is carried out by considering different coefficient of variation (CV) values by varying the standard deviation. A comparative study of computational time needed for the execution of perturbation approach and MCS is also done.

In the next section, for the benefit of the reader, a brief description of BSWI and its properties is given.

B-spline wavelet on the interval [0, 1]

The theory of spline wavelets for whole square integrable real space $L^2(\mathbf{R})$ was developed by

Chui and Wang [17–19]. Wavelets defined on $L^2(\mathbf{R})$ cannot be directly used as interpolating functions as it results in numerical instability [20]. Hence, Chui and Quak [10] addressed this issue by constructing wavelet bases for the bounded interval [0, 1], which came to be known as BSWI. Spline wavelets are semi-orthogonal wherein, they retain inter-scale orthogonality and there is no necessity for the basis functions to be orthogonal to its translates within the same resolution level. By introducing multiple knots at the endpoints, splines can readily adapt to the case of the bounded interval [0, 1]. As a result, no truncation is needed when the function on $L^2(\mathbf{R})$ is restricted. By way of suitable adaptation at the endpoints, MRA of $L^2(\mathbf{R})$ can be implemented over to [0, 1]. Multiple knots exist at end points (0 and 1 in the case of BSWI) and they do not diminish the overall order of smoothness of the elements on [0, 1]. The continuity of B-splines depends on the selected order m in such a way that B-splines with order m are in C_{m-2} continuity. The analytical expressions for the BSWI scaling functions ϕ and wavelet functions ψ for given order m and resolution $j=0$ can be found in the paper by Goswami et al. [21] and the expressions for order m and any resolution j were given by Xiang et al. [12] as,

$$\phi_{m,k}^{j}(\xi) = \left\{ \begin{array}{l} \phi_{m,k}^{l}(2^{j-l}\xi), \quad k=-m+1,...,-1, \ \text{(0 boundary scaling functions)} \\ \phi_{m,2^j-m-k}^{l}(1-2^{j-l}\xi), \quad k=2^j-m+1,...,2^j-1, \\ \text{(1 boundary scaling functions)} \\ \phi_{m,0}^{l}(2^{j-l}\xi-2^{-l}k), \quad k=0,...,2^j-m, \ \text{(inner scaling functions)} \end{array} \right\} \tag{1}$$

$$\psi_{m,k}^{j}(\xi) = \left\{ \begin{array}{l} \psi_{m,k}^{l}(2^{j-l}\xi), \quad k=-m+1,...,-1, \ \text{(0 boundary wavelets)} \\ \psi_{m,2^j-2m-k+1}^{l}(1-2^{j-l}\xi), \quad k=2^j-2m+2,...,2^j-m \\ \text{(1 boundary wavelets)} \\ \psi_{m,0}^{l}(2^{j-l}\xi-2^{-l}k), \quad k=0,...,2^j-2m+1, \ \text{(inner wavelets)} \end{array} \right\} \tag{2}$$

The compactly supported intervals of wavelets are,

$$\text{supp}\ \psi_{m,k}^{j}(\xi) = \left\{ \begin{array}{l} [0,\ (2m-1+k)2^{-j}], \ \text{(0 boundary wavelets)} \\ [k2^{-j},\ 1], \ \text{(1 boundary wavelets)} \\ [k2^{-j},\ (2m-1+k)2^{-j}], \ \text{(inner wavelets)} \end{array} \right\} \tag{3}$$

BSWI scaling functions are categorized as the boundary scaling functions that exist at boundary points 0 and 1 on the domain and inner scaling functions that are dilations and translations of cardinal B-splines as shown in Eq. (1), (2) and (3). Eventually, the corresponding wavelets can be constructed from the scaling functions. BSWI scaling functions of different order and resolution which are used in the current study are shown in Figure 1.

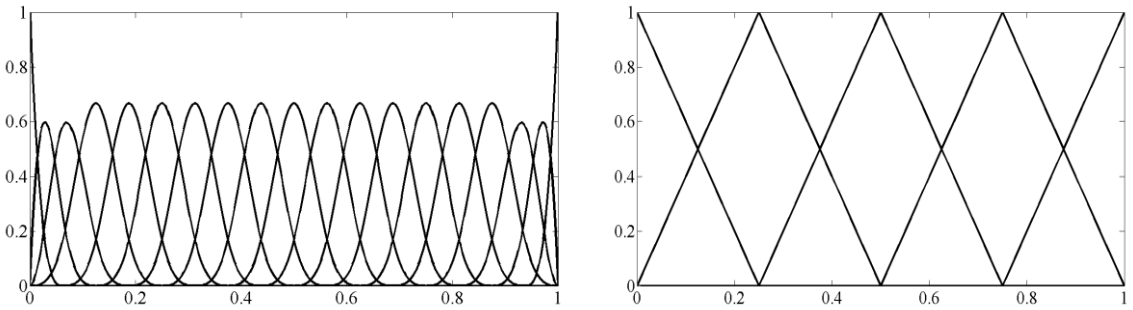

a) $m = 4,\ j = 4$ b) $m = 2,\ j = 2$

Figure 1.BSWI scaling functions using different order and resolution

Formulation of stochastic BSWI WFEM element for elastic buckling of columns

In BSWI WFEM, the problem domain Ω is divided into sub-domains Ω_i (i=1, 2...) and each Ω_i is then mapped into the standard element solving domain $\Omega_e = \{\xi \mid \xi \in [0, 1]\}$, where instead of using the traditional polynomial interpolation, scaling or scaling and wavelet functions of BSWI can be used to form the shape functions over the elements Ω_e. Here ξ is the local co-ordinate used for solving 1D BSWI on [0, 1] along y axis.

Deterministic modelling

The generalized functional of potential energy governing static buckling of columns is given as [22],

$$\prod = \frac{1}{2}\int_0^L EI\left(\frac{d^2 w_0}{dx^2}\right)^2 dx - \frac{P}{2}\int_0^L \left(\frac{dw_0}{dx}\right)^2 dx \tag{4}$$

Here, w_0 is the transverse deflection, I is the second moment of area, P is the axial compressive load, E is the Young's modulus. One BSWI WFEM beam element based on Euler-Bernoulli theory (EBT) which was developed by Xiang et al. [12] is used in the present study. One BSWI EBT beam element with C_1 continuity is divided into $2^j + m - 3$ nodes with end nodes having both transverse and rotational degrees of freedom (DOF) and internal nodes having only transverse DOF as shown in Figure 2, where m, j are the order and resolution of BSWI scaling functions respectively.

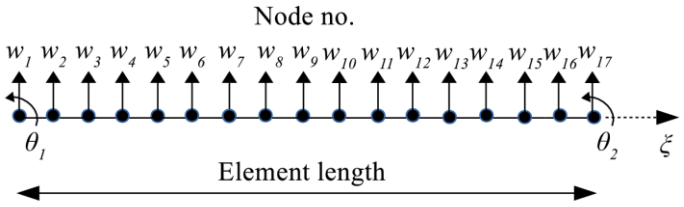

Figure 2.Distribution of nodes and degrees of freedom for one BSWI EBT based beam element with C_1 continuity using $m = 4,\ j = 4$

The unknown transverse deflection field function of Euler-Bernoulli beam element is approximated in the element solving domain ξ in terms of wavelet scaling functions as,

$$w_0(\xi) = \sum_{k=-m+1}^{2^j-1} b^j{}_{m,k}\phi^j{}_{m,k}(\xi) = \boldsymbol{\varphi}\boldsymbol{b}^{\boldsymbol{e}} \tag{5}$$

where, $\boldsymbol{\varphi} = \{\phi^j{}_{m,-m+1}(\xi).....\phi^j{}_{m,2^j-1}(\xi)\}$ is the row vector of BSWI scaling functions and $\boldsymbol{b}^{\boldsymbol{e}} = \{b^j{}_{m,-m+1}\, b^j{}_{m,-m+2}....b^j{}_{m,2^j-1}\}^T$ is the column vector of wavelet coefficients that needs to be determined. The unknown transverse deflection field function can be expressed in terms of C_1 element type transformation matrix and physical DOF as,

$$w_0(\xi) = \boldsymbol{\varphi}(\boldsymbol{R}^{\boldsymbol{e}})^{-1}\boldsymbol{w}^{\boldsymbol{e}} = \boldsymbol{\varphi}\,\boldsymbol{T}^{\boldsymbol{e}}\boldsymbol{w}^{\boldsymbol{e}} = \boldsymbol{N}^{\boldsymbol{e}}\boldsymbol{w}^{\boldsymbol{e}} \tag{6}$$

where,

$$\left.\begin{aligned}
&\boldsymbol{w}^{\boldsymbol{e}} = \left\{ w_1\ \theta_1\ w_2\ w_3.....w_n\ w_{n+1}\ \theta_{n+1} \right\}^T, \\
&\theta_1 = \frac{1}{l_e}\left(\frac{dw_0(\xi_1)}{d\xi}\right), \theta_{n+1} = \frac{1}{l_e}\left(\frac{dw_0(\xi_{n+1})}{d\xi}\right), \\
&l_e = x_{n+1} - x_1,\ \boldsymbol{w}^{\boldsymbol{e}} = \boldsymbol{R}^{\boldsymbol{e}}\boldsymbol{b}^{\boldsymbol{e}},\ \boldsymbol{T}^{\boldsymbol{e}} = (\boldsymbol{R}^{\boldsymbol{e}})^{-1}, \\
&\boldsymbol{R}^{\boldsymbol{e}} = \left[\boldsymbol{\varphi}^T(\xi_1)\ \ \frac{1}{l_e}\left(\frac{d\boldsymbol{\varphi}^T(\xi_1)}{d\xi}\right)\ \ \boldsymbol{\varphi}^T(\xi_2).....\boldsymbol{\varphi}^T(\xi_n)\ \ \boldsymbol{\varphi}^T(\xi_{n+1})\ \ \frac{1}{l_e}\left(\frac{d\boldsymbol{\varphi}^T(\xi_{n+1})}{d\xi}\right) \right]^T, \\
&\boldsymbol{N}^{\boldsymbol{e}} = \boldsymbol{\varphi}\,\boldsymbol{T}^{\boldsymbol{e}}
\end{aligned}\right\} \tag{7}$$

The elemental transformation matrix transforms the stiffness matrix from wavelet space into physical space. The transformation matrix also maintains the continuity and compatibility within the element and by using an assembly matrix, at the interface between the neighbouring elements. Upon substituting the deflection field of Eq. (6) into the weak form and invoking the stationary condition for variation of admissible deflections, the solution of static buckling of columns is obtained in the form of an Eigen value problem as,

$$\left(\boldsymbol{K}^{e} - \boldsymbol{P}\boldsymbol{G}^{e}\right)\boldsymbol{w}^{e} = 0 \tag{8}$$

where,

$$\left.\begin{aligned} \boldsymbol{K}^{e} &= \frac{EI}{\left(l_{ex}\right)^{3}}\int_{0}^{1}\left(\boldsymbol{T}^{e}\right)^{T}\left(\frac{d^{2}\boldsymbol{\varphi}}{d\xi^{2}}\right)^{T}\left(\frac{d^{2}\boldsymbol{\varphi}}{d\xi^{2}}\right)\left(\boldsymbol{T}^{e}\right)d\xi\ , \\ \boldsymbol{G}^{e} &= \frac{1}{l_{ex}}\int_{0}^{1}\left(\boldsymbol{T}^{e}\right)^{T}\left(\frac{d\boldsymbol{\varphi}}{d\xi}\right)^{T}\left(\frac{d\boldsymbol{\varphi}}{d\xi}\right)\left(\boldsymbol{T}^{e}\right)d\xi \end{aligned}\right\} \tag{9}$$

Here, $\boldsymbol{K}^{e}$ is the elemental stiffness matrix and $\boldsymbol{G}^{e}$ is the elemental geometric stiffness matrix. The Eigen values $\boldsymbol{P}$ from Eq. (8) correspond to the buckling loads and the Eigen vectors $\boldsymbol{w}^{e}$ correspond to the mode shapes.

Stochastic modelling

In the present work, the Young's modulus $E(\mathbf{x})$ is considered as a spatially varying homogeneous lognormal random field. As a result, the generalized functional of total potential as given in Eq. (4) along with response, will also become stochastic in nature. When $E(\mathbf{x})$ is a homogeneous lognormal field with mean μ_{E_l} and standard deviation σ_{E_l} it can be expressed in terms of $\alpha(\mathbf{x})$ as,

$$E(\mathbf{x}) = C_l e^{\alpha(\mathbf{x})} \tag{10}$$

with

$$C_l = \frac{\mu_{E_l}^{2}}{\sqrt{\mu_{E_l}^{2} + \sigma_{E_l}^{2}}} \tag{11}$$

The auto-covariance kernel for $\alpha(\mathbf{x})$ can be written as [23],

$$\Gamma_{\alpha_l} = \ln\left(1 + \frac{\sigma_{E_l}^{2}}{\mu_{E_l}^{2}}\right)\exp\left[-\left(\Sigma_{i}^{n}\frac{|\Delta_i|}{c_i}\right)\right] \tag{12}$$

where, $n \in \mathbf{R}^{n}$, Δ_i is the distance between two points x_a, x_b along i, c_i is the correlation length parameter which determines the statistical correlation of field variable in the domain. Here, $\alpha(\mathbf{x})$ is a random field that does not possess an explicit expression and hence requires an approximation, which can be achieved by approximating a function over a set of random variables distributed in the domain obtained by discretization of the random field. In the current study, for modelling the random field a shape function method is proposed to be used.

Shape function method using Lagrange interpolation and moving least square shape functions has been employed in SFEM [24] and stochastic meshless methods [6] respectively. However, in the present study, BSWI scaling functions are used to model both the random field and response.

On similar lines, as the deflection field is approximated in Eq. (5), the unknown random field can be approximated in the element solving domain in terms of BSWI scaling functions as,

$$\alpha(\xi) = \sum_{k=-m_r+1}^{2^{j_r}-1} b^{j_r}{}_{m_r,k}\phi^{j_r}{}_{m_r,k}(\xi) = \boldsymbol{\varphi}_{\mathrm{R}}\boldsymbol{b}_{\mathrm{R}}^{e} \tag{13}$$

where, $\boldsymbol{\varphi}_{\mathrm{R}} = \{\phi^{j_r}{}_{m_r,-m_r+1}(\xi).....\phi^{j_r}{}_{m_r,2^{j_r}-1}(\xi)\}$ is the row vector of BSWI scaling functions, $\boldsymbol{b}_{\mathrm{R}}^{e} = \{b^{j_r}{}_{m_r,-m_r+1}\, b^{j_r}{}_{m_r,-m_r+2}....b^{j_r}{}_{m_r,2^{j_r}-1}\}^{T}$ is the column vector of wavelet coefficients that needs to be determined and m_r , j_r are the order and resolution of BSWI scaling function chosen for the discretization of random field. The subscript r is used here to denote the function or variable associated with the random field. Also, it can be noted that the order and resolution that is used for the discretization of the deflection field and random field can be different from each other. The unknown random field function is expressed in terms of C_0 element type transformation matrix as,

$$\alpha(\xi) = \boldsymbol{\varphi}_{\mathrm{R}}\left(\boldsymbol{R}_{\mathrm{R}}^{e}\right)^{-1}\boldsymbol{\alpha}_{\mathrm{R}}^{e} = \boldsymbol{\varphi}_{\mathrm{R}}\boldsymbol{T}_{\mathrm{R}}^{e}\boldsymbol{\alpha}_{\mathrm{R}}^{e} = \boldsymbol{N}_{\mathrm{R}}^{e}\boldsymbol{\alpha}_{\mathrm{R}}^{e} \tag{14}$$

where, $\boldsymbol{\alpha}_{\mathrm{R}}^{e} = \left\{\alpha_{1\mathrm{R}}\ \alpha_{2\mathrm{R}}.....\alpha_{(n+1)\mathrm{R}}\right\}^{T}$ is the set random variables distributed over the domain of the element. Thus, element stiffness coefficients and hence the element deflections will become functions of random variables $\boldsymbol{\alpha}_{\mathrm{R}}^{e}$ and Eq. (8) becomes a stochastic Eigen value problem as,

$$\left[\boldsymbol{K}^{e}\left(\boldsymbol{\alpha}_{\mathrm{R}}^{e}\right) - \boldsymbol{P}\left(\boldsymbol{\alpha}_{\mathrm{R}}^{e}\right)\boldsymbol{G}^{e}\right]\boldsymbol{w}^{e}\left(\boldsymbol{\alpha}_{\mathrm{R}}^{e}\right) = 0 \tag{15}$$

When $E(\mathbf{x})$ is modelled as a homogeneous lognormal field as given in Eq. (10), the $\boldsymbol{K}^{e}$ in Eq. (15) can be written as,

$$\boldsymbol{K}^{e} = \frac{\mu_{E_l} I}{\left(l_{ex}\right)^{3}\sqrt{1+\left(\dfrac{\sigma_{E_l}}{\mu_{E_l}}\right)^{2}}}\left\{\int_{0}^{1}\exp^{\left(\boldsymbol{\varphi}_{\mathrm{R}}\boldsymbol{T}_{\mathrm{R}}^{e}\boldsymbol{\alpha}_{\mathrm{R}}^{e}\right)}\left(\boldsymbol{T}^{e}\right)^{T}\left(\frac{d^{2}\boldsymbol{\varphi}}{d\xi^{2}}\right)^{T}\left(\frac{d^{2}\boldsymbol{\varphi}}{d\xi^{2}}\right)\left(\boldsymbol{T}^{e}\right)d\xi\right\} \tag{16}$$

Here, $\boldsymbol{K}^{e}$ is the elemental stochastic stiffness matrix for beams based on EBT formulation. The element stiffness matrices $\boldsymbol{K}^{e}$ and $\boldsymbol{G}^{e}$ are obtained for all the sub-domains and assembled together to obtain the global stochastic Eigen value problem as,

$$\left[\boldsymbol{K}\left(\boldsymbol{\alpha}_{\mathrm{R}}\right)-\boldsymbol{P}\left(\boldsymbol{\alpha}_{\mathrm{R}}\right)\boldsymbol{G}\right]\boldsymbol{W}\left(\boldsymbol{\alpha}_{\mathrm{R}}\right)=0 \tag{17}$$

From Eq. (17), the second moment characteristics of buckling loads (Eigen values) $\boldsymbol{P}$ and mode shapes $\boldsymbol{w}$ (Eigen vectors) are obtained using the perturbation method which is discussed in the next section.

Perturbation method

Perturbation method uses the expansion of the global stiffness matrix $\boldsymbol{K}$, Eigen values $\boldsymbol{P}$ and Eigen vectors $\boldsymbol{w}$ via Taylor series [8]. It is based on the assumption that the variance of the random field should be small. Let $\Lambda=\{\alpha_i\}_{i=1}^{N}$ denote the vector of N zero mean random variables representing the random field in the global domain Ω. The Taylor series expansion of $\boldsymbol{K}$, $\boldsymbol{P}$ and $\boldsymbol{w}$ can be obtained as,

$$\boldsymbol{K}=\boldsymbol{K}_0+\sum_{i=1}^{N}\boldsymbol{K}_i^{I}\boldsymbol{\alpha}_i+\frac{1}{2}\sum_{i=1}^{N}\sum_{j=1}^{N}\boldsymbol{K}_{ij}^{II}\boldsymbol{\alpha}_i\boldsymbol{\alpha}_j+....,\Bigg\} \tag{18}$$

$$\boldsymbol{P}=\boldsymbol{P}_0+\sum_{i=1}^{N}\boldsymbol{P}_i^{I}\boldsymbol{\alpha}_i+\frac{1}{2}\sum_{i=1}^{N}\sum_{j=1}^{N}\boldsymbol{P}_{ij}^{II}\boldsymbol{\alpha}_i\boldsymbol{\alpha}_j+.....,\Bigg\} \tag{19}$$

$$\boldsymbol{W}=\boldsymbol{W}_0+\sum_{i=1}^{N}\boldsymbol{W}_i^{I}\boldsymbol{\alpha}_i+\frac{1}{2}\sum_{i=1}^{N}\sum_{j=1}^{N}\boldsymbol{W}_{ij}^{II}\boldsymbol{\alpha}_i\boldsymbol{\alpha}_j+.....,\Bigg\} \tag{20}$$

where, $\boldsymbol{K}_0$, $\boldsymbol{P}_0$, $\boldsymbol{W}_0$ are deterministic values evaluated at $\boldsymbol{K}(0),\boldsymbol{P}(0),\boldsymbol{W}(0)$; $(.)_i^{I}=\dfrac{\partial(.)}{\partial\boldsymbol{\alpha}_i}(0)$, and $(.)_{ij}^{II}=\dfrac{\partial^2(.)}{\partial\boldsymbol{\alpha}_i\partial\boldsymbol{\alpha}_j}(0)$. Upon substituting Eq. (18), (19) and Eq. (20) into Eq. (17) and rearranging the terms of the same order gives,

$$\left[\boldsymbol{K}_0-\boldsymbol{P}_0\boldsymbol{G}\right]\boldsymbol{W}_0=0 \tag{21}$$

$$\left[\boldsymbol{K}_0-\boldsymbol{P}_0\boldsymbol{G}\right]\boldsymbol{W}_i^{I}+\left[\boldsymbol{K}_i^{I}-\boldsymbol{P}_i^{I}\boldsymbol{G}\right]\boldsymbol{W}_0=0 \tag{22}$$

$$\left[\boldsymbol{K}_0-\boldsymbol{P}_0\boldsymbol{G}\right]\boldsymbol{W}_{ij}^{II}+\left[\boldsymbol{K}_i^{I}-\boldsymbol{P}_i^{I}\boldsymbol{G}\right]\boldsymbol{W}_j^{I}+\left[\boldsymbol{K}_j^{I}-\boldsymbol{P}_j^{I}\boldsymbol{G}\right]\boldsymbol{W}_i^{I}+\left[\boldsymbol{K}_{ij}^{II}-\boldsymbol{P}_{ij}^{II}\boldsymbol{G}\right]\boldsymbol{W}_0=0 \tag{23}$$

It is to be noted that $\boldsymbol{K}_0-\boldsymbol{P}_0\boldsymbol{G}$ is symmetric, which leads to,

$$\left[\boldsymbol{K}_0-\boldsymbol{P}_0\boldsymbol{G}\right]=\left[\boldsymbol{K}_0-\boldsymbol{P}_0\boldsymbol{G}\right]^{T} \tag{24}$$

Pre-multiplying Eq. (22) and (23) by $\boldsymbol{W}_0^{T}$ and using Eq. (24) leads to,

$$\left[\left(\boldsymbol{K}_0-\boldsymbol{P}_0\boldsymbol{G}\right)\boldsymbol{W}_0\right]^{T}\boldsymbol{W}_i^{I}+\boldsymbol{W}_0^{T}\left[\boldsymbol{K}_i^{I}-\boldsymbol{P}_i^{I}\boldsymbol{G}\right]\boldsymbol{W}_0=0 \tag{25}$$

$$\left[\left(\boldsymbol{K}_0 - \boldsymbol{P}_0\boldsymbol{G}\right)\boldsymbol{W}_0\right]^T \boldsymbol{W}_{ij}^{II} + \boldsymbol{W}_0{}^T\left[\boldsymbol{K}_i^I - \boldsymbol{P}_i^I\boldsymbol{G}\right]\boldsymbol{W}_j^I + \boldsymbol{W}_0{}^T\left[\boldsymbol{K}_j^I - \boldsymbol{P}_j^I\boldsymbol{G}\right]\boldsymbol{W}_i^I + \boldsymbol{W}_0{}^T\left[\boldsymbol{K}_{ij}^{II} - \boldsymbol{P}_{ij}^{II}\boldsymbol{G}\right]\boldsymbol{W}_0 = 0 \tag{26}$$

Upon simplification of Eq. (25) leads to,

$$\boldsymbol{P}_i^I = \left[\boldsymbol{W}_0{}^T\boldsymbol{G}\boldsymbol{W}_0\right]^{-1}\left[\boldsymbol{W}_0{}^T\boldsymbol{K}_i^I\boldsymbol{W}_0\right] \tag{27}$$

By substituting Eq. (27) into Eq. (25), $\boldsymbol{W}_i^I$ can be obtained, which can be further substituted into Eq. (26) to obtain,

$$\boldsymbol{P}_{ij}^{II} = \left[\boldsymbol{W}_0{}^T\boldsymbol{G}\boldsymbol{W}_0\right]^{-1}\left(\boldsymbol{W}_0{}^T\left[\boldsymbol{K}_i^I - \boldsymbol{P}_i^I\boldsymbol{G}\right]\boldsymbol{W}_j^I + \boldsymbol{W}_0{}^T\left[\boldsymbol{K}_j^I - \boldsymbol{P}_j^I\boldsymbol{G}\right]\boldsymbol{W}_i^I + \boldsymbol{W}_0{}^T\boldsymbol{K}_{ij}^{II}\boldsymbol{W}_0\right) \tag{28}$$

Upon the substitution of Eq. (28) into Eq. (26) $\boldsymbol{W}_{ij}^{II}$ can be obtained. By applying the expectation and variance operators on the first order or second order approximation of Eq. (19), the first and second order statistics of critical buckling load can be obtained as,

First order approximation

$$\left.\begin{aligned} \mu_{P_{cr}} &= \boldsymbol{P}_0 \quad , \\ \gamma_{P_{cr}} &= \sum_{i=1}^{N}\sum_{j=1}^{N}\boldsymbol{P}_i^I\left(\boldsymbol{P}_j^I\right)^T\Gamma_{\alpha}(\alpha_i,\alpha_j) \end{aligned}\right\} \tag{29}$$

Second order approximation

$$\left.\begin{aligned} \mu_{P_{cr}} &= \boldsymbol{P}_0 + \frac{1}{2}\sum_{i=1}^{N}\sum_{j=1}^{N}\boldsymbol{P}_{ij}^{II}\,\Gamma_{\alpha}(\alpha_i,\alpha_j) \ , \\ \gamma_{P_{cr}} &= \sum_{i=1}^{N}\sum_{j=1}^{N}\boldsymbol{P}_i^I\left(\boldsymbol{P}_j^I\right)^T\Gamma_{\alpha}(\alpha_i,\alpha_j) + \\ &\frac{1}{4}\sum_{i=1}^{N}\sum_{j=1}^{N}\sum_{k=1}^{N}\sum_{l=1}^{N}\boldsymbol{P}_{ij}^{II}\left(\boldsymbol{P}_{kl}^{II}\right)^T\left\{\Gamma_{\alpha}(\alpha_i,\alpha_l)\Gamma_{\alpha}(\alpha_j,\alpha_k) + \Gamma_{\alpha}(\alpha_i,\alpha_k)\Gamma_{\alpha}(\alpha_j,\alpha_l)\right\} \end{aligned}\right\} \tag{30}$$

Similarly statistics of other response functions of interest, like $\boldsymbol{W}$ can also be found out. In the next section, a few 1D numerical examples are solved based on the preceding formulations and the results are analysed.

Numerical examples

Two numerical examples are solved with the proposed stochastic BSWI WFEM formulation for elastic buckling of columns. Columns with pinned-pinned (p-p) and fixed-pinned (f-p) boundary conditions under axial compressive loading as shown in Figure 3 are considered for the study. The response statistics for buckling loads and mode shapes are calculated via perturbation approach and the results are compared with the statistics obtained from MCS. From a convergence study, based on the calculation of relative percentage error

in L_2 norm of mean and standard deviation values of Young's modulus for various MCS sample size; it is noted that an error of less than 1% is obtained when the MCS sample size is 5000. Hence, MCS sample size of 5000 is considered in the current study. The mean value of Young's modulus is taken as $\mu_{E_l} = 2\times10^5$ MPa with L = 100 mm, $b = 1$mm and $h = 1$mm. The entire domain of the column is modelled using one BSWI C_1 type continuity element. The deflection field is approximated using cubic ($m = 4$) BSWI scaling functions with a resolution of $j = 4$ and the random field is approximated with linear ($m = 2$) BSWI scaling functions with a coarse resolution of $j = 2$.

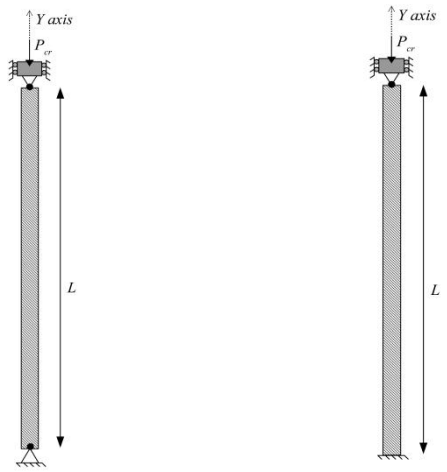

a) Pinned-Pinned b) Fixed-Pinned

Figure 3.Columns with various boundary conditions under axial compressive loading

The mean values of the buckling loads (first, second and third) for a pinned-pinned (p-p) column obtained by using the perturbation approach are shown in Figure 4. These values are compared with the values obtained from MCS and the results are plotted for different values of CV, obtained by varying the standard deviation of Young's modulus $E(\mathbf{x})$. The correlation length parameter considered is 50. It can be observed from Figure 4 that at a CV of 20% the results obtained from perturbation approach are in good agreement with MCS for all the buckling loads. However, at a CV of 25%, a deviation of 3% is observed between the perturbation and MCS results in the case of third buckling load. The variation of standard deviation values of buckling loads against CV are shown in Figure 5. It can be observed that even at a CV of 25%, the values obtained from perturbation approach concur well with the MCS values for all the buckling loads.

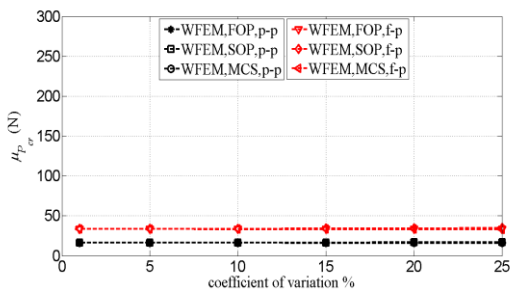

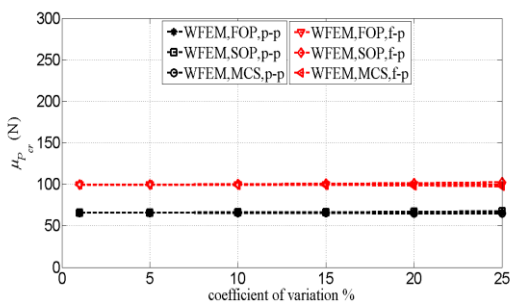

a) First buckling load b) Second buckling load

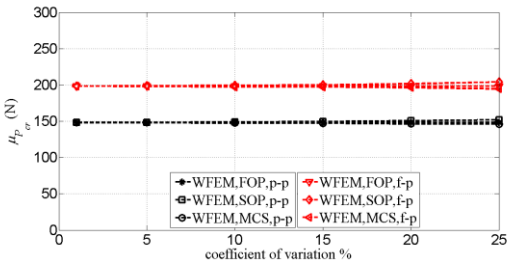

c) Third buckling load

Figure 4.Variation of mean values of buckling loads for columns with different boundary conditions against CV

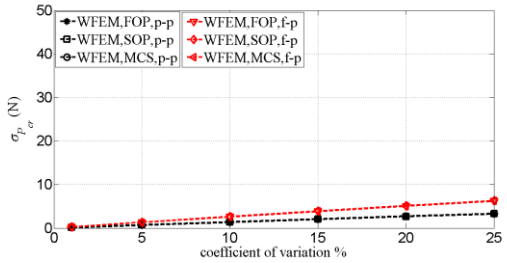

a) First buckling load

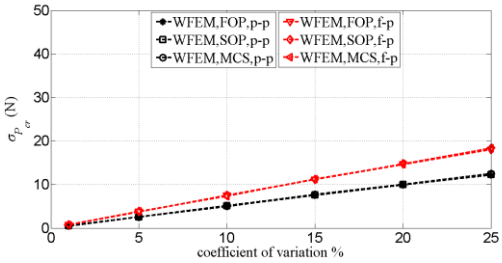

b) Second buckling load

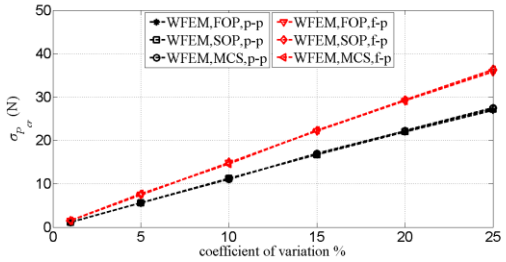

c) Third buckling load

Figure 5.Variation of standard deviation values of buckling loads for columns with different boundary conditions against CV

The variation of mean and standard deviation values of buckling loads obtained by using the perturbation approach against varying correlation length parameter is shown in Figure 6 and Figure 7 respectively. A value of 5% is considered for CV during the process. Figure 6 and 7 shows that even at a small correlation length parameter the values obtained from WFEM based perturbation approach remain in good agreement with the MCS values. This shows that a coarse discretization of random field using BSWI WFEM is able to accurately capture the results even at extreme correlation length parameters unlike SFEM, wherein the dependency of correlation length parameter on random field mesh is well documented [3,24] and would require a higher number of random variables to be used for accurate results.

Besides the buckling loads, the first three mode shapes are also plotted for the pinned-pinned column in Figure 8. It can be seen that WFEM based perturbation approach accurately captures the first three mode shapes when compared with MCS results.

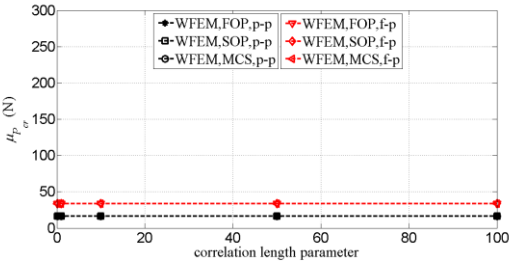

a) First buckling load

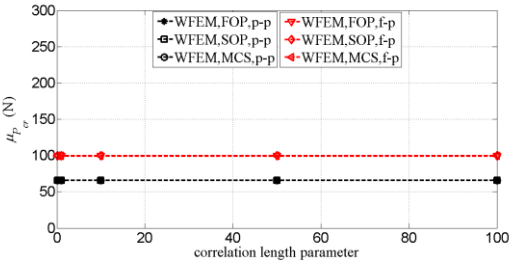

b) Second buckling load

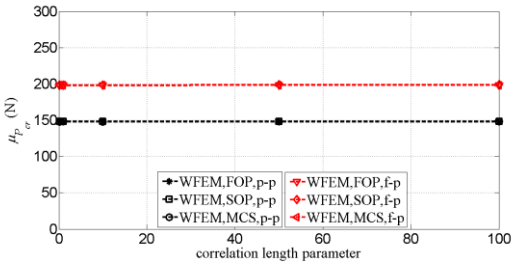

c) Third buckling load

Figure 6.Variation of mean values of buckling loads for columns with different boundary conditions against correlation length parameter

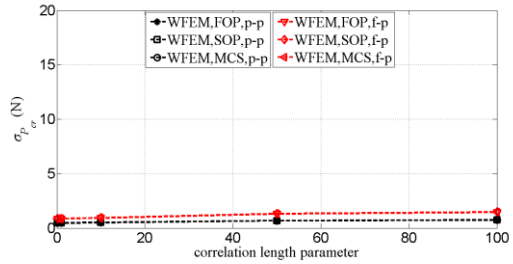

a) First buckling load

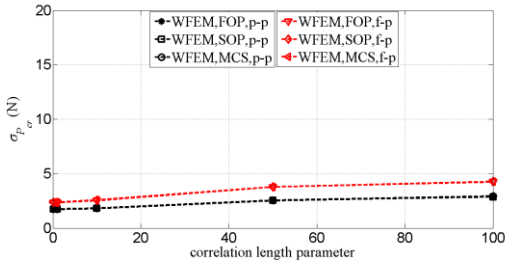

b) Second buckling load

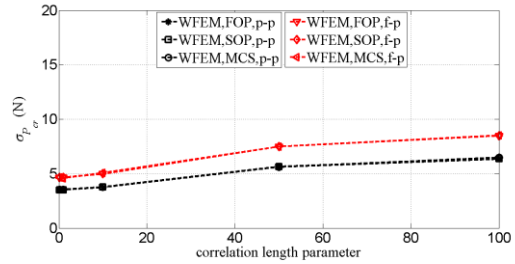

c) Third buckling load

Figure 7.Variation of standard deviation values of buckling loads for columns with different boundary conditions against correlation length parameter

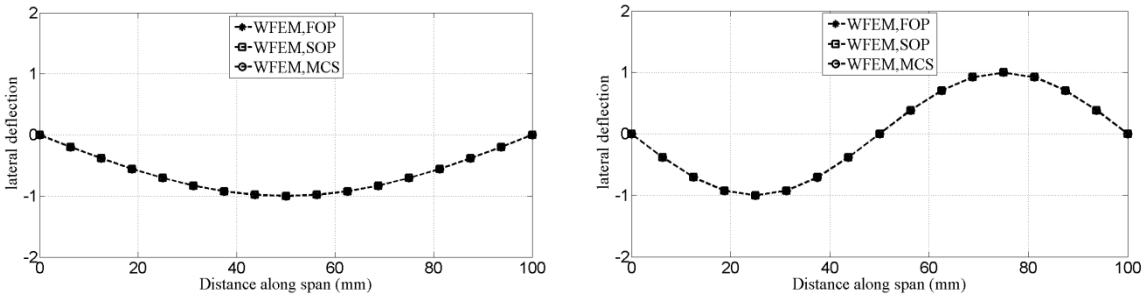

a) First mode

b) Second mode

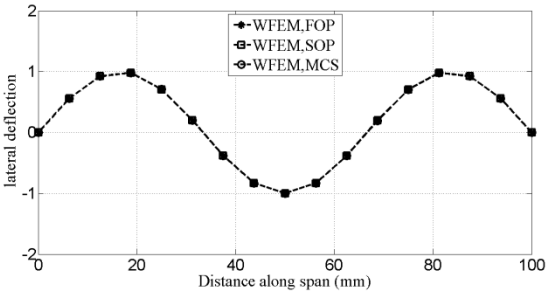

c) Third mode

Figure 8. Mode shapes for a pinned-pinned column

The mean values of the buckling loads for a fixed-pinned (f-p) column obtained by using the perturbation approach are shown in Figure 4. It can be observed from Figure 4 that at a CV of 25% there is a deviation of around 5% between the results obtained from perturbation approach and MCS for the third buckling load. However, no such deviation is observed in the standard deviation values obtained from perturbation approach and MCS as seen in Figure 5. Similar to the case of pinned-pinned columns, the mean and standard deviation values of buckling loads against varying correlation length parameters for a fixed-pinned column show a good agreement between the perturbation and MCS results as observed in Figure 6 and Figure 7. Furthermore, the first three mode shapes as shown in Figure 9 reinstates the accuracy of the WFEM based perturbation approach.

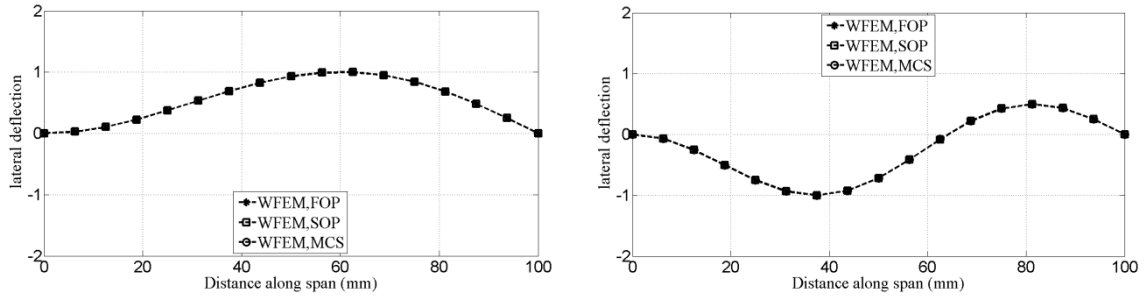

a) First mode b) Second mode

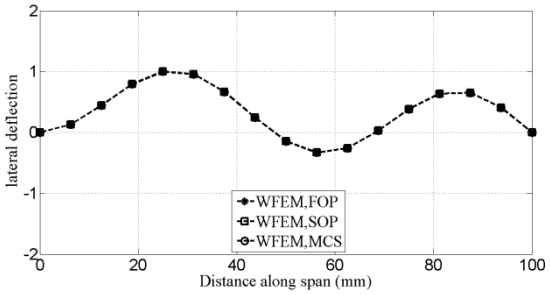

c) Third mode

Figure 9. Mode shapes for a fixed-pinned column

Computational time

Besides evaluating the mean and standard deviation values of the buckling loads, the normalized computational times required by the perturbation approach (FOP and SOP combined) and MCS (5000 simulations) is also calculated. It is noted that in the case of a pinned-pinned column, the execution time of MCS is 39.63 times more in comparison with WFEM based perturbation approach. Similarly, for a fixed-pinned column, the execution time of MCS is 38.28 times more than the perturbation method. Hence, the proposed BSWI WFEM based perturbation approach is not only accurate but also computationally more efficient in comparison with the MCS based approach.

Conclusion

The current paper proposes the formulation of stochastic BSWI WFEM formulation for elastic buckling of columns wherein, the spatial variation of modulus of elasticity is modelled as a homogeneous random field. In the present work, BSWI scaling functions are used for the approximation of deflection field as well as random field. The response statistics are calculated using the perturbation approach and validated by comparing with the results of MCS. The results obtained from the numerical examples show that WFEM based perturbation approach can be used to accurately capture the response statistics of the buckling load for values of CV up to 25%.

The domain of the column is discretized using only one BSWI WFEM element, due to which, there are no meshes and the programming effort needed in the pre-processing stage to form a global matrix from the assembly of multiple elements is reduced. The parametric study on correlation length parameters show that the values obtained from perturbation approach based on WFEM concur well with MCS values at extremely small or large correlation length parameters even when the random field is modelled using a coarse nodal discretization. Further, the normalized computational times are calculated for both the numerical examples and WFEM based perturbation approach takes less time in comparison with MCS in both the cases, thereby making it more efficient.

References

[1] Bauchau, O. A., and Craig, J. I., *Structural Analysis With Applications to Aerospace Structures*, Springer.

[2] Choi, S.-K., Grandhi, R. V, and Canfield, R. A., 2007, *Reliability-Based Structural Design*, Springer London.

[3] Stefanou, G., 2009, "The Stochastic Finite Element Method: Past, Present and Future," Comput. Methods Appl. Mech. Eng., **198**(9–12), pp. 1031–1051.

[4] Vanmarcke, E., and Grigoriu, M., 1983, "Stochastic Finite Element Analysis of Simple Beams," J. Eng. Mech., **109**(5), pp. 1203–1214.

[5] Lin, S. C., and Kam, T. Y., 1992, "Buckling Analysis of Imperfect Frames Using a Stochastic Finite Element Method," Comput. Struct., **42**(6), pp. 895–901.

[6] Rahman, S., and Rao, B. N., 2001, "A Perturbation Method for Stochastic Meshless Analysis in Elastostatics," Int. J. Numer. Methods Eng., **50**(8), pp. 1969–1991.

[7] Rahman, S., and Xu, H., 2005, "A Meshless Method for Computational Stochastic Mechanics," Int. J. Comput. Methods Eng. Sci. Mech., **6**(1), pp. 41–58.

[8] Gupta, A., and Arun, C. O., 2018, "Stochastic Meshfree Method for Elastic Buckling Analysis of Columns," Comput. Struct., **194**, pp. 32–47.

[9] Li, B., and Chen, X., 2014, "Wavelet-Based Numerical Analysis: A Review and Classification," Finite Elem. Anal. Des., **81**, pp. 14–31.

[10] Chui, C. K., and Quak, E., 1992, "Wavelets on a Bounded Interval," *Numerical Methods in Approximation Theory, Vol. 9*, Birkhäuser Basel, Basel, pp. 53–75.

[11] Chui, C. K., 1992, *An Introduction to Wavelets - Wavelet Analysis and Its Applications*, Academic press.

[12] Xiang, J. W., Chen, X. F., He, Z. J., and Dong, H. B., 2007, "The Construction of 1D Wavelet Finite Elements for Structural Analysis," Comput. Mech., **40**(2), pp. 325–339.

[13] Zuo, H., Yang, Z. B., Chen, X. F., Xie, Y., Zhang, X. W., and Liu, Y., 2014, "Static, Free Vibration and Buckling Analysis of Functionally Graded Beam via B-Spline Wavelet on the Interval and Timoshenko Beam Theory," C. - Comput. Model. Eng. Sci., **100**(6), pp. 477–506.

[14] Zuo, H., Yang, Z., Chen, X., Xie, Y., and Zhang, X., 2014, "Bending, Free Vibration and Buckling Analysis of Functionally Graded Plates via Wavelet Finite Element Method," C. Comput. Mater. Contin., **44**(3), pp. 167–204.

[15] Yang, Z., Chen, X., Zhang, X., and He, Z., 2013, *Free Vibration and Buckling Analysis of Plates Using B-Spline Wavelet on the Interval Mindlin Element*, Appl. Math. Model.

[16] Elishakoff, I., 1979, "Buckling of a Stochastically Imperfect Finite Column on a Nonlinear Elastic Foundation: A Reliability Study," J. Appl. Mech., **46**(2), p. 411.

[17] Chui, C. K., and Wang, J., 1991, "A Cardinal Spline Approach to Wavelets," Proc. Am. Math. Soc., **113**(3), p. 785.

[18] Chui, C. K., and Wang, J.-Z., 1992, "On Compactly Supported Spline Wavelets and a Duality Principle," Trans. Am. Math. Soc., **330**(2), pp. 903–915.

[19] Chui, C. K., and Wang, J. Z., 1993, "An Analysis of Cardinal Spline-Wavelets," J. Approx. Theory, **72**(1), pp. 54–68.

[20] Bertoluzza, S., Naldi, G., and Ravel, J. C., 1994, "Wavelet Methods for the Numerical Solution of Boundary Value Problems on the Interval," *Wavelets: Theory, Algorithms, and Applications*, C.K. Chui, and Others, eds., pp. 425–448.

[21] Goswami, J. C., Chan, A. K., and Chui, C. K., 1995, *On Solving First-Kind Integral Equations Using Wavelets on a Bounded Interval*, IEEE Trans.

[22] Bathe, K. J., 2010, *Finite Element Procedures*, PHI learning private limited, {New} {Delhi}.

[23] Xu, H., and Rahman, S., 2005, "Decomposition Methods for Structural Reliability Analysis," Probabilistic Eng. Mech., **20**(3), pp. 239–250.

[24] Sudret, B., and Kiureghian, A. Der, 2000, *Stochastic Finite Element Methods and Reliability: A State-of-the-Art Report*.